Journal of Catalysis **198,** 286–295 (2001)
doi:10.1006/jcat.2000.3131, available online at http://www.idealibrary.com on IDEAL®

The Nature of the Active Metal Surface of Catalysts for the Clean Combustion of Biogas Containing Ammonia

R. Burch[1] and B. W. L. Southward

School of Chemistry, Queen's University Belfast, Belfast, BT9 5AG, Northern Ireland, United Kingdom

Received August 28, 2000; revised October 30, 2000; accepted November 20, 2000; published online February 8, 2001

The nature of the active surface of supported metal catalysts for the clean combustion of ammonia-containing simulated biogas has been investigated to understand the very high N_2 selectivity of some catalysts. A comparison of the activities of Al_2O_3-supported precious group metals has shown that under conventional operating conditions the fuel is fully combusted but NH_3 is converted predominantly into NO_x. In contrast, it is shown that it is possible by operating under O_2-deficient conditions to attain essentially zero emissions of NO_x with Rh- or Ir-based catalysts, whereas Pt or Pd gave markedly lower selectivities to N_2. These variations in selectivity are attributed to the differences in the state of the metal surface during reaction. For Rh- and Ir-based catalysts it has been shown that under fuel-rich conditions, surface carbon, derived from the dissociative adsorption of CO, results in self-poisoning toward CO and H_2 oxidation at low temperatures. However, at higher temperatures a preference toward methanation of the C_{ads} is observed. It is thought that this surface reaction between the C_{ads} and H_{ads} scavenges both reductants so that O_{ads} can react with NH_3 in a highly specific manner, to give NO_x. The NO_x thus formed is subsequently reduced by reaction with excess CO to give N_2. A model is presented that shows the way in which the chemistry of the surface of the active metal changes as the reaction parameters are varied.

Key Words: **gasified biomass; biogas; heterogeneous catalyst; selective NH_3 oxidation.**

INTRODUCTION

Potential problems with CO_2 emissions and the associated "Greenhouse Effect" are well documented (1) and have resulted in a growing interest in developing cleaner, renewable energy sources (2, 3). Biomass represents an interesting alternative energy source and work is in progress to try to commercialize gasified biomass (biogas), produced from partial oxidation/pyrolysis of biosolids, as a primary fuel for combined heat and power generation (CHP) (4–19). The fuel component of this biogas comprises about 9.8–17.2% CO and 9.8–13.2% H_2 and additional light hydrocarbons, e.g., CH_4 (4). However, biogas also contains significant quantities of NH_3 (600–4000 ppm), derived from biogenic organonitrogen compounds (4). The NH_3, formed during the gasification of these species, presents a particular challenge since its combustion in a conventional suspended flame burner results in the formation of a significant amount of nitrogen oxides (NO_x) which are also subject to emissions legislation (20–22).

Eliminating NO_x emissions from the combustion of biogas poses significant technical challenges. A range of approaches have been proposed, including: water scrubbing of the gasification stream (23); *in situ* catalytic methods of selective oxidation to N_2 (5–16); NH_3 decomposition (by conventional and membrane reactors) (17–19); and selective noncatalytic or catalytic reduction of the tail gas postcombustion (24, 25). However, all these methods have significant drawbacks. Water scrubbing is effective for ammonia removal but creates a wastewater disposal problem. Similarly, treatment of the NO_x-containing exhaust gas with NH_3 in a conventional NH_3-selective catalytic reduction (SCR) reactor is effective but has high associated costs and process limitations. In contrast, while both *in situ* catalytic and noncatalytic methods are less expensive and do not require secondary disposal or cleanup systems, they provide only limited N_2 selectivities even under idealized laboratory conditions, i.e., comparatively low gas hourly space velocities (GHSVs) and CO/H_2 levels (6–11).

In addition, the mechanism of N_2 formation in these processes is still uncertain. Various authors have claimed that N_2 formation arises as a result of the condensation of an oxidized N species with a reduced N species (12, 13, 15, 16, 26–32). This reaction has recently been dubbed internal selective catalytic reduction (iSCR) and has been shown to occur on metal oxides, heteropoly acids, and zeolitic catalysts, giving very high N_2 selectivities (12, 13, 15, 16, 32). In contrast, Ramis and co-workers (33, 34) have suggested, based on FTIR studies, that NH_3 oxidation to N_2 involves a hydrazinium-type intermediate. More recently it has also been claimed that N_2 formation during biogas oxidation is in fact a homogeneous gas-phase reaction, involving a selective noncatalytic reduction (SNCR) of NO by NH_3

[1] To whom correspondence should be addressed. Fax: +44 (0) 2890 27 4687. E-mail: r.burch@qub.ac.uk.

0021-9517/01 $35.00

(7, 9). Conversely, Johansson and Järås ascribed high N_2 production over a Ni–Al_2O_3 catalyst to gas-phase reduction of NO by the hydrocarbons present in the fuel. However, the same study reported identical activity for the blank reactor system, again indicating that the contribution of homogeneous chemistry may be significant (8).

Under real commercial conditions the problem is even more intractable because it has also been found that the efficiency of many of the laboratory-based *in situ* catalytic systems is further compromised by the presence of sulfur, alkalis, and other contaminants in the biogas stream (10, 11, 17). Moreover, catalytic activity for the selective oxidation of NH_3 is also inhibited in the presence of high concentrations of the fuel components (CO and H_2) (16).

In the present work we have adopted a novel approach to the problem of selective oxidation. The basic challenge is to achieve a *double* selectivity in oxidation of a typical simulated biogas mixture under a variety of reaction conditions. It is necessary to achieve selective oxidation of NH_3 in the presence of large excesses of CO and H_2. However, it is also necessary to achieve selective conversion of the NH_3 to N_2 rather than to NO_x. Thus the aim of our work has been to develop materials and methodologies capable of meeting the low NO_x emissions targets required for a biogas-driven CHP turbine, i.e., operation at high GHSV in the presence of high concentrations of CO/H_2.

EXPERIMENTAL

Catalyst Preparation

All catalysts were prepared by incipient wetness impregnation of the dried support (Akzo CK300, Al_2O_3 surface area 195 $m^2\ g^{-1}$) using nitrate (Ag, Cu, and Rh), DNDA (Pt), and $Ir(CH_3COCH{=}C(O)CH_3)_3$ precursors to give the nominal loadings indicated. All samples were dried at room temperature (24 h), then at 120°C (24 h) prior to calcination at 700°C (12 h) in static air.

Performance Evaluation

Catalyst testing was performed using a standard plug-flow microreactor described previously (12). The sample (60 mg, 425–800 μm) was held between plugs of quartz wool in a quartz tubular horizontal flow reactor (i.d. 5 mm) and supported by a hollow quartz rod. The reactor was heated in a furnace with temperatures being maintained to ±1°C by a Eurotherm 818p controller. The reactant gases, 1% NH_3 in He, 60 : 40 CO/H_2, 100% CO, 100% H_2, 1% O_2 in He, 20% O_2 in He, pure O_2, 5000 ppm NO in He, and He, were supplied through electronic mass flow controllers. Water was added using an Instech Model 2000 syringe pump. Unless otherwise stated, total flow was 300 $cm^3\ min^{-1}$ (corresponding to a GHSV of ca. 240,000 h^{-1}) with a feed composition of 1000 ppm NH_3 and fuel and O_2 levels as indicated. Product analysis was performed by mass spectrometry (Hiden DSMS) and by an external NH_3 oxidation reactor (equipped with a Pt–Al_2O_3 catalyst and independent O_2 supply) coupled to a Signal Series 4000 chemiluminescence detector for determination of NO, total NO_x (defined as $NO + NO_2$), and residual NH_3 emissions.

Temperature-programmed oxidation (TPO), reduction (TPR), desorption (TPD), and reaction (TPRe), were performed *in situ* using the equipment described above, at a ramp of 12°C min^{-1} and total gas flow of 300 $cm^3\ min^{-1}$. All samples were purged for 30 min in He prior to analysis. BET surface areas were determined by N_2 adsorption using apparatus built in-house.

RESULTS

Lean Oxidation of NH_3 and $NH_3/CO/H_2$ Mixtures

The problem in obtaining high selectivity for the oxidation of NH_3 to N_2 under lean (oxygen rich) conditions has been noted in the Introduction. Figure 1, which compares the oxidation of NH_3 over a range of Al_2O_3-supported metal catalysts, illustrates this point. In all cases the N_2 selectivity decreased markedly with temperature, with parallel increases in NO_x production. Of the various materials tested 1% Cu–Al_2O_3 displayed the highest N_2 yield (>90% at 450°C). This was expected because under these conditions N_2 production has been shown to arise via an iSCR mechanism (8–10, 26–32) and Cu-based catalysts are known to be effective for the NH_3/NO SCR reaction (23, 24). However, as has been noted already for both Al_2O_3-supported base and precious metal catalysts (9, 12, 26) the temperature

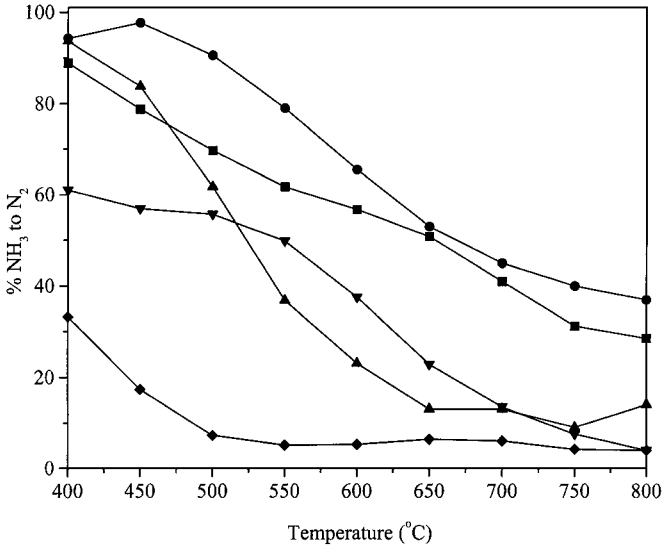

FIG. 1. N_2 yields for the selective catalytic oxidation of NH_3 over 1% metal–Al_2O_3 catalysts (1000 ppm NH_3, 18% O_2, balance He). ■, Ag; ●, Cu; ▼, Pd; ◆, Pt; ▲, Rh.

range over which high N_2 selectivity is observed is very limited. This may be a consequence of the iSCR mechanism in which oxidation of NH_3 to NO_x has to be carefully balanced by reduction of the NO_x with unreacted NH_3 (9, 10, 24).

The corresponding lean oxidation reactions of a $NH_3/CO/H_2$ mixture (1000 ppm NH_3, 1.02% CO, 0.68% H_2, 18% O_2) revealed similar trends with reduced N_2 yields so the results are not reproduced here. The reduction in N_2 selectivity and the increase in the formation of NO are ascribed to competition for surface sites, with the CO and H_2 competing for O_{ads}. In addition, exothermic effects due to the combustion of the CO and H_2 can cause the surface temperature to be significantly raised. Figure 1 shows that this would also result in a loss of selectivity to N_2 (12, 13, 15, 16, 26–32). These results, and those of other studies (6–10, 17, 18) emphasize the problems with the conventional approach to NH_3 oxidation in biogas streams.

Rich Oxidation of $NH_3/CO/H_2$ and NO/CO Mixtures

The limited success of the conventional oxidation reaction described above led us to propose an alternative strategy to overcome NO_x production. We adopted an integrated solution in which the fuel components of the reaction mixture were used, in conjunction with process control, to overcome NO_x formation. Thus we investigated catalysts that could completely oxidize NH_3 to NO_x under fuel-rich conditions. In this approach we anticipated that the NO_x thus formed could be reduced very easily by residual CO, H_2, or even NH_3 all of which have previously been demonstrated (24, 25, 35–37). Thus the challenge was to selectively oxidize NH_3 in the presence of a large excess of CO and H_2.

To investigate this possibility, the activity of 2% Rh–Al_2O_3 for NH_3 oxidation (1000 ppm NH_3, 2175 ppm O_2, at 400°C) was examined in the absence and presence of CO (10,000 ppm). Figure 2 shows that under CO-free conditions NH_3 conversion was 100% (trace ●), but only at the expense of high NO production (trace △), which was approximately 240 ppm, i.e., ca. 24% yield of NO_x. When CO was introduced, NO was no longer detected by MS or NO_x measurements. However, the NH_3 conversion was unaffected by the presence of CO, and since no NO_x was detected, we can conclude that we have achieved quantitative conversion of NH_3 into N_2. Finally, when CO was replaced by He, the catalyst rapidly reattained its previous steady-state activity with high NO_x (>95% as NO) production again being observed.

These results may be contrasted with those obtained using 1% Pt–Al_2O_3 (data not shown). In this case the introduction of CO resulted in a significant amount of NH_3 slipping through unreacted. Presumably, although the Pt can oxidize NH_3 rapidly in the absence of CO, this reaction is not as competitive with CO oxidation on Pt as it is on Rh. On removal of the CO, catalyst activity was restored to original levels, i.e., ca. 100% NH_3 conversion and a high selectivity for NO formation (ca. 700 ppm, i.e., 70% yield).

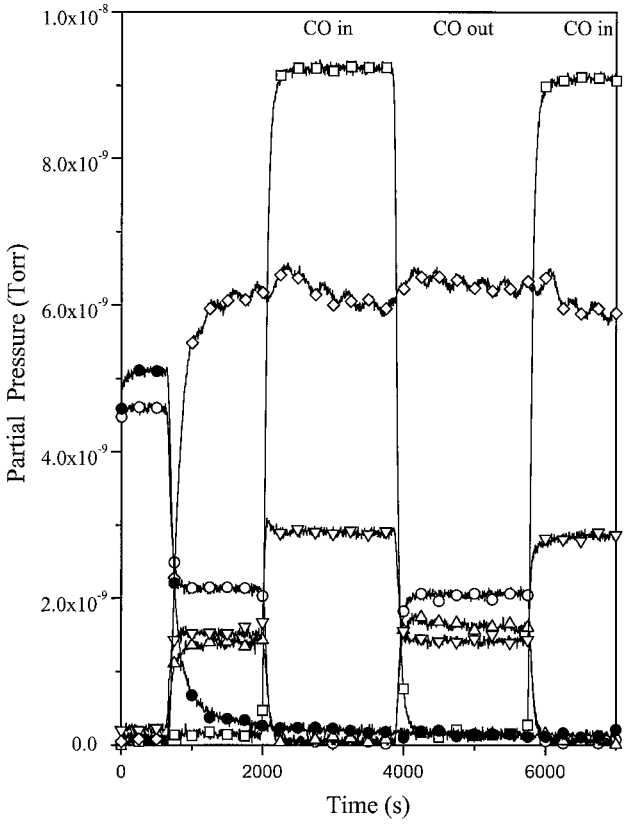

FIG. 2. Effect of CO/He switches on the activity of a 2% Rh–Al_2O_3 catalyst for the selective catalytic oxidation of NH_3 (400°C, 1000 ppm NH_3, 2175 ppm O_2, 10,000 ppm CO switched in/out, balance He). □, *m/z* 44 (CO_2, N_2O); ○, *m/z* 32 (O_2); △, *m/z* 30 (NO); ▽, *m/z* 28 (CO/N_2); ◇, *m/z* 18 (H_2O); ●, *m/z* 16 (NH_3).

We conclude from these experiments that Rh and Pt are fundamentally different in the way they interact with NH_3/CO mixtures. A crucial feature of the Rh is that it seems to be able to differentiate between NH_3 and CO so that the NH_3 is selectively oxidized, with respect to CO, even in the presence of excess of CO. Subsequently, the NO/CO or NO/NH_3 reactions, or a combination of both, can account for the high selectivity to N_2. This was confirmed by examining the activity of the 2% Rh–Al_2O_3 catalyst for the reduction of NO by a combination of CO and H_2 under rich conditions (1000 ppm NO, 1.02% CO, 0.68% H_2, 0.275% O_2, data not shown). In this case the NO/CO/H_2 reaction was found to be facile, with 100% NO conversion to N_2 observed at $T \geq 210$°C, in agreement with previously published data (24, 35, 37, 38). Thus, we conclude that the oxidation of NH_3 to NO, rather than the reduction of NO by CO, H_2, and/or residual NH_3, is the limiting factor in our coupled reaction method.

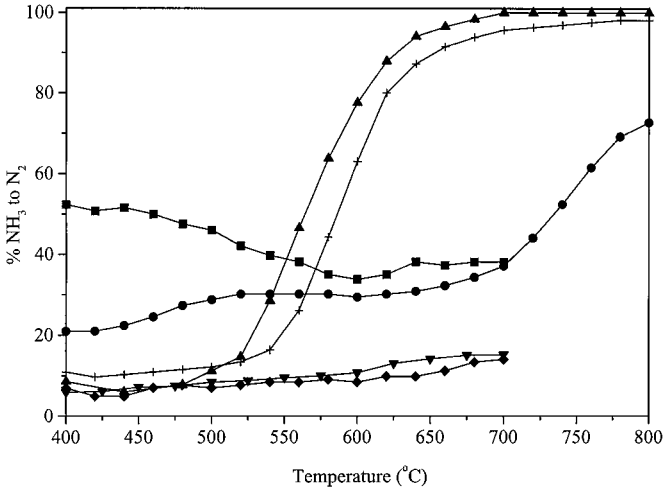

FIG. 3. NH_3-to-N_2 conversion profiles for the O_2 lean combustion of simulated biogas over 1% metal–Al_2O_3 catalysts (1000 ppm NH_3, 0.275% O_2, 1.02% CO, 0.68% H_2, balance He). ■, Ag; ●, Cu; +, Ir; ▼, Pd; ◆, Pt; ▲, Rh.

To follow up the observed differences in performance between Rh and Pt we have examined other supported metal catalysts. Fig. 3 shows that quantitative production of N_2 was possible using the coupled reaction method with Rh- or Ir-based materials. Conversely, N_2 yields over Pt- and Pd-based materials were low, while Cu gave an increasing yield at higher temperatures and Ag produced ca. 50% N_2 at 400–475°C. Clearly, Ir has properties comparable to those of Rh whereas Pd is similar to Pt. This may reflect the inherent affinity of Rh and Ir for CO, compared with Pt or Pd, with a concomitant tendency for dissociative adsorption.

MS analysis of the reaction over 1% Rh–Al_2O_3 (Fig. 4) corroborates the NO_x results regarding NH_3 conversion (traces ▼, Fig. 4a and 4b without NO formation (trace ▲, Fig. 4b). Analysis of the data also revealed a complex interplay between CO, H_2, and O_2. For example, initial H_2 combustion increased in the region from 450 to 525°C before decreasing. Significantly the sharp decrease in H_2 combustion, starting at ca. 525°C, occurred simultaneously with the onset of NH_3 conversion, suggesting there is competition between H_2 and NH_3 for the available O_2. Conversely, the initial amount of CO_2 produced was approximately equal to that of H_2O below 500°C but increased markedly at $T > 500$°C. The low-temperature feature is ascribed to a combination of CO oxidation and CO disproportion (39), and the high-temperature reaction to the oxidation of CH_4 (see below) and reduction of CO by NO, the latter being formed from NH_3 oxidation. Finally, above 525°C, the curve for *m/z* 16 (CH_4/80% of NH_3, trace ▼) revealed a temperature response different from that for *m/z* 17 (NH_3), this difference being ascribed to methanation of CO-derived species by H_2 with a distinct maximum at 600°C. Again it should be noted that onset of CH_4 formation, i.e., the preference of H_2 for CO-derived species rather than for oxidation by O_{ads}, occurred at the same temperature as the onset of N_2 formation.

Temperature-Programmed Studies

To further examine the role of competitive adsorption in biogas oxidation, temperature-programmed studies were performed (Figs. 5–7). These may be summarized as follows. First, it was found that the adsorption and reactivity of NH_3 were strongly influenced by the presence of O_2. Thus, in TPO (Fig. 5, filled symbols) there was concomitant production/desorption of N_2, N_2O, and NO at ca. 300°C, consistent with the proposed iSCR (8–10, 26–32). Conversely, in TPD (reducing conditions) (Fig. 5, open symbols) there was no production/desorption of NO or N_2O over the entire temperature range and N_2 production was lower with a desorption maximum some 75°C higher. These observations

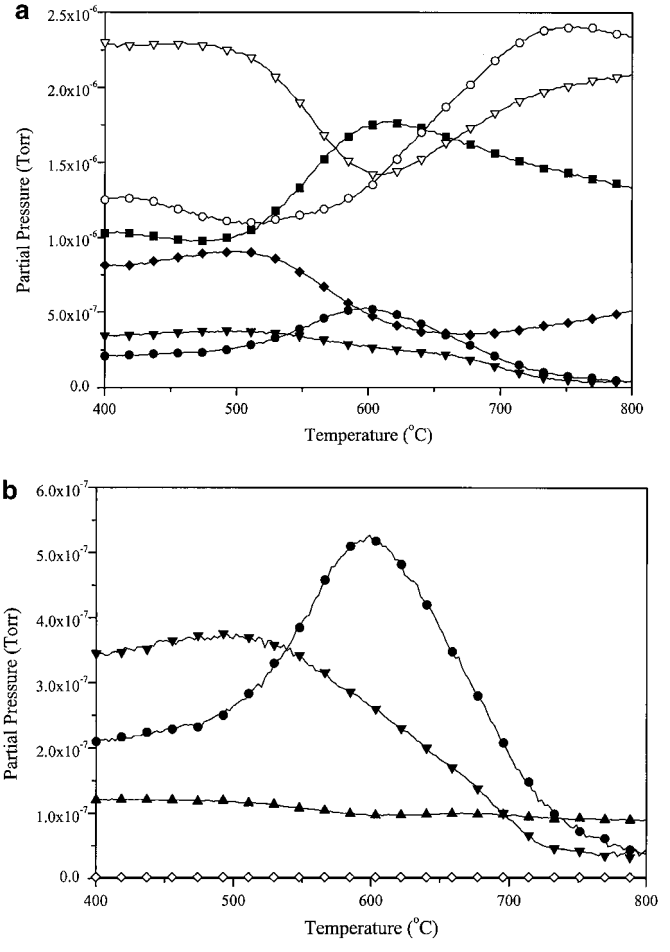

FIG. 4. Conversion profiles for the O_2 lean combustion of simulated biogas over 1% Rh–Al_2O_3 (1000 ppm NH_3, 0.275% O_2, 1.02% CO, 0.68% H_2, balance He). (a) Major products: ■, *m/z* 44; ▽, *m/z* 28; ◆, *m/z* 18; ▼, *m/z* 17; ●, *m/z* 16; ○, *m/z* 2. (b) Minor products: ◇, *m/z* 32; ▲, *m/z* 30 ∗ 10; ▼, *m/z* 17; ●, *m/z* 16.

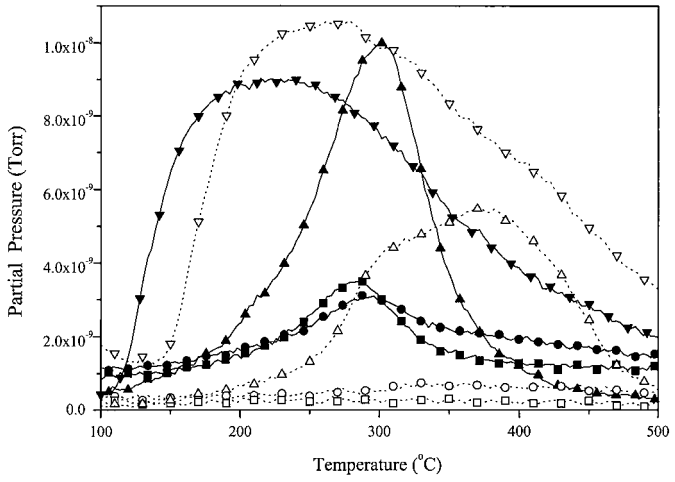

FIG. 5. Temperature-programmed oxidation/desorption from 2% $Rh–Al_2O_3$. (catalysts dosed at 100°C with either 1000 ppm NH_3 or 1000 ppm NH_3, 0.275% O_2, balance He and ramped in He or 0.275% O_2 in He). □, *m/z* 44/N_2O (TPD); ○, *m/z* 30/NO (TPD); △, *m/z* 28/N_2 (TPD); ▽, *m/z* 17/NH_3 (TPD); ■, *m/z* 44/N_2O (TPO); ●, *m/z* 30/NO (TPO); ▲, *m/z* 28/N_2 (TPO); ▼, *m/z* 17/NH_3 (TPO).

are consistent with a process in which NH_3 reacts with the limited amount of O_2 on the catalyst (26–30).

The adsorptive properties of the 2% $Rh–Al_2O_3$ were completely altered by the presence of CO and H_2 during dosing (Fig. 6), with these changes paralleling the differences seen in steady-state kinetic studies. Hence when CO and H_2 were present during dosing, NO was not detected over the entire temperature range, consistent with the preferential reduction of the catalyst by CO or H_2 and the consequent blocking of the "typical" iSCR process for the formation of N_2.

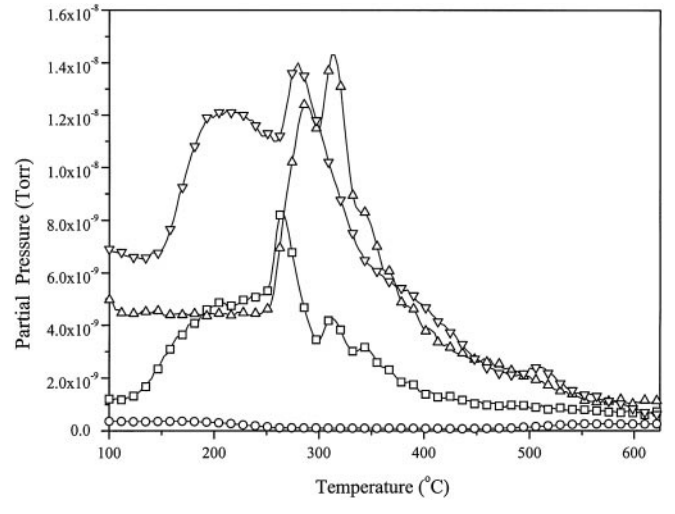

FIG. 6. Temperature-programmed desorption of $CO/H_2/NH_3$ mixture from 2% $Rh–Al_2O_3$ (catalyst dosed at 100°C with 1000 ppm NH_3, 1.02% CO, 0.68% H_2, balance He). □, *m/z* 44/N_2O/CO_2; ○, *m/z* 30/NO; △, *m/z* 28/CO/N_2; ▽, *m/z* 17/NH_3.

The possible blockage of some of the Rh surface by CO-derived species was further investigated by TPR analysis of catalysts removed from the reaction (ex-reactor catalysts). Separate samples of 1% $Rh–Al_2O_3$ were used to catalyze the $NH_3/CO/H_2/O_2$ reaction (1000 ppm NH_3, 5.1% CO, 3.4% H_2, 0.26% O_2) at 400, 615, and 750°C. Effluent analysis after 1 h on-line gave NH_3 to N_2 yields of ca. 5, 25, and 98%, respectively. The samples were then cooled to 200°C in a He purge and subsequently heated in flowing H_2 (5% in He) and the production of CH_4 was monitored, giving the results shown in Fig. 7a.

For the ex-400°C reaction case, substantial amounts of CH_4 were recorded in peaks at 440 and 500°C. However, for the ex-615°C case the lower-temperature features in the TPR were lost and the high-temperature CH_4 peak was significantly reduced in size, while the ex-750°C sample exhibited no CH_4 production. The presence of a C-containing

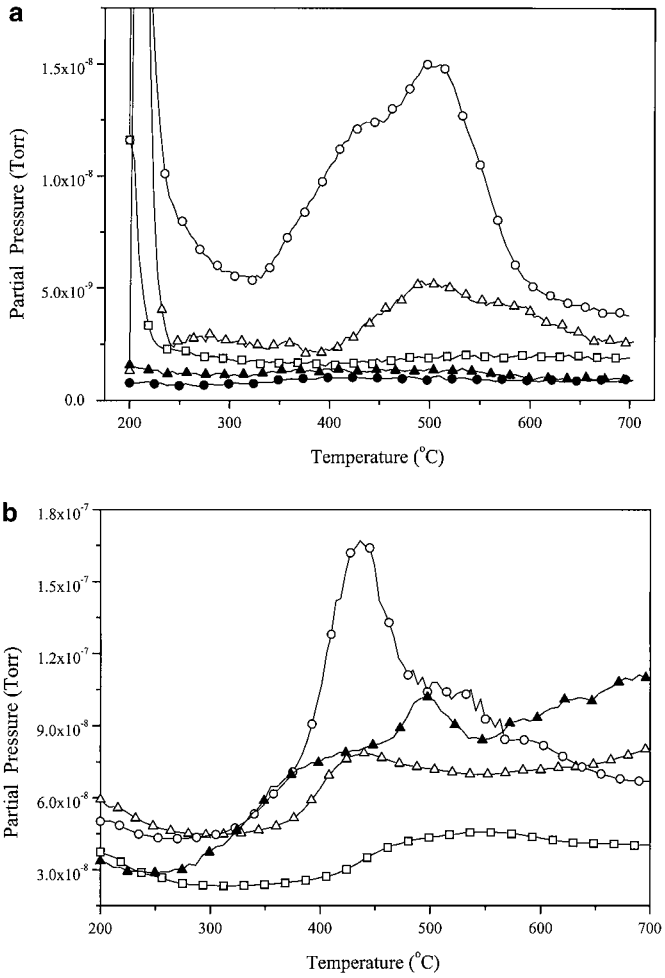

FIG. 7. Temperature-programmed reduction of 1% $Rh–Al_2O_3$ and 1% $Pt–Al_2O_3$ ex-$NH_3/CO/H_2/O_2$ reaction (1000 ppm NH_3, 0.26% O_2, 5.1% CO, 3.4% H_2, balance He). (a) CH_4 peaks: ○, Rh ex 400°C; △, Rh ex 615°C; □, Rh ex 750°C; ●, Pt ex 400°C; ▲, Pt ex 615°C. (b) H_2O peaks: ○, Rh ex 400°C; △, Rh ex 615°C; □, Rh ex 750°C; ▲, Pt ex 615°C.

species was corroborated by TPO of an ex-615°C catalyst which exhibited a corresponding CO_2 peak at approximately 500°C (not shown). Collectively these results show that the surface of the Rh is modified in the presence of CO, probably through the deposition of C_{ads}, to the extent that oxidation of NH_3 can occur selectively even under fuel-rich conditions. This seems to be key to the success of our methodology with Rh (and Ir) catalysts. The Rh results are in marked contrast to those obtained with the 1% Pt–Al_2O_3 catalyst.

Analysis of H_2O production during TPR (Fig. 7b) also reflected the differences between the three Rh samples, with the ex-615 and ex-750°C materials exhibiting only small high-temperature H_2O peaks, consistent with dehydroxylation of the Al_2O_3 rather than reduction of O-containing species as seen ex-400°C. Thus it is clear in these cases that there is a gradual loss of $CO_{(ads)}$-derived species with temperature. Moreover, the data suggest that these moieties are removed via a two-stage process giving first H_2O and second CH_4, identical to the trends observed during rich NH_3 oxidation (Fig. 4b). Conversely for 1% Pt–Al_2O_3 all the H_2O profiles were identical (Fig. 7b shows ex-615°C).

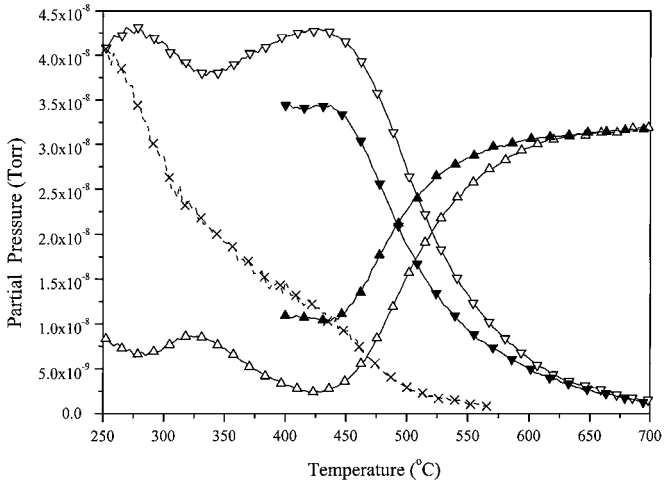

FIG. 8. MS profiles for the $NH_3/H_2/O_2$ and $NH_3/CO/O_2$ reactions over 1% Rh–Al_2O_3 (1000 ppm NH_3, 0.275% O_2, 1% H_2 or CO, balance He). Fresh catalyst ex $NH_3/H_2/O_2$: ▽, *m/z* 16/NH_3, △, *m/z* 28/N_2. Aged catalyst ex $NH_3/H_2/O_2$ (aged in 1000 ppm NH_3, 5.1% CO, 3.4% H_2, 0.275% O_2 at 400°C for 1 h): ▼, *m/z* 16/NH_3; ▲, *m/z* 28/N_2. Fresh catalyst ex $NH_3/CO/O_2$ ×, *m/z* 16/NH_3.

Comparison of the $H_2/NH_3/O_2$ and $CO/NH_3/O_2$ Reactions

The earlier results suggest that a C_{ads}-type species on Rh (or Ir) could be important in controlling the reactivity. Consequently, under similar fuel-rich conditions, where CO is replaced by H_2, we might expect to see different results. Therefore, we compared the performance of 1% Rh–Al_2O_3 in the $NH_3/H_2/O_2$ and $NH_3/CO/O_2$ reactions. The results are summarized in Fig. 8. In the case of the $NH_3/CO/O_2$ reaction, full NH_3 conversion, with 100% selectivity to N_2 (determined via NO_x analysis), is attained at ca. 550°C, some 150°C lower than the temperature required in the $NH_3/H_2/O_2$ case. Moreover, it was found that while increasing CO levels to 2% somewhat suppressed activity (100% NH_3 to N_2 at 600°C), further increases in CO concentration to 4 and 8% had no appreciable impact on activity. These results are broadly comparable to those obtained in the switching experiments (Fig. 2) if we take account of the lower Rh concentration and the detrimental effects of CO adsorption below the light-off temperature (ca. 275°C), which result in partial poisoning of the catalyst.

The presence of CO-derived species was also found, at least on a temporary basis, to promote the activity of the Rh catalyst in the $H_2/NH_3/O_2$ reaction. Figure 8 also compares the activities of fresh 1% Rh–Al_2O_3 and 1% Rh–Al_2O_3 after pretreatment in an $NH_3/CO/H_2/O_2$ mixture (1 h at 400°C, 1000 ppm, 5.1%, 3.4%, 0.275%). Hence at 400°C it was noted that both NH_3 conversion and N_2 production post-CO exposure were higher (cf. traces △ for fresh, ▲ for ex-CO), with quantitative analysis by chemiluminescence giving values of 29 and 6% N_2, respectively. However as the temperature of the reaction increased the activities of the samples converged, as might be expected due to loss of adsorbed C-containing species (see Fig. 8).

In contrast, H_2 has a major negative effect on the NH_3-to-N_2 reaction. Thus when trace amounts of H_2 (500 ppm) were introduced into the $NH_3/CO/O_2$ system (1000 ppm NH_3/4% CO/0.275% O_2 at 450°C) after 180 s, Fig. 9 shows that there are corresponding increases in the signals at *m/z* 2, *m/z* 18, and *m/z* 17, consistent with the increased level of H_2 in the system and increased water production from H_2 oxidation. However, this results in a corresponding decrease in the combustion of NH_3 due to O_2 depletion and a

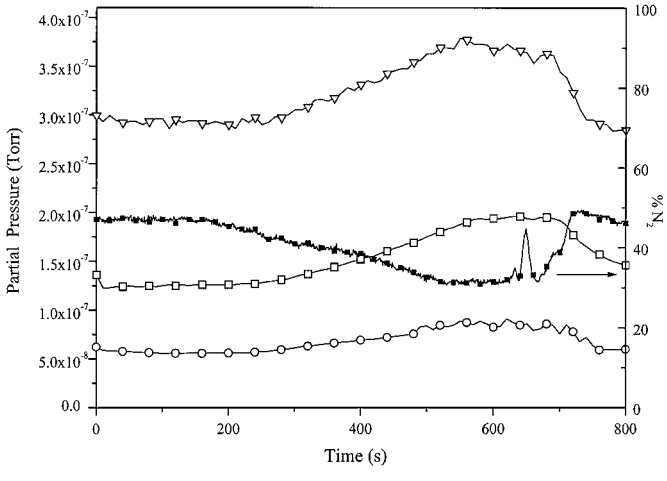

FIG. 9. Effect of H_2 (500 ppm) on the activity of 1% Rh–Al_2O_3 in the $NH_3/CO/O_2$ reaction at 450°C (1000 ppm NH_3, 4% CO, 0.275% O_2). ▽, *m/z* 2; ○, *m/z* 17; □, *m/z* 18 (∗5); ■, NH_3 to N_2 from NO_x analysis (on *Y*2 axis).

decrease in N_2 production, as corroborated by NO_x analysis. When the H_2 is switched off (seen as a spike in trace ■) the catalyst recovers its activity over 60 s, suggesting that a CO-derived species can accumulate on the Rh surface again on this time scale.

Mechanistic Aspects: A Comparison of NO/NH_3, CO/NO, and NH_3 Decomposition Reactions

Examination of the possible pathways for N_2 production from NH_3 oxidation indicates that there are four possible pathways to N_2 production within the system. These fall into two classes. The first is a the coupled oxidation–reduction route in which NO is formed from NH_3 and subsequently reduced by (i) NH_3, (ii) CO, or (iii) H_2, and the second is NH_3 decomposition. To determine the major pathway of N_2 production we have compared the rates of these various reactions, giving the results summarized in Fig. 10. These data indicate that the NO/CO reaction is most kinetically favored in the absence of competing reactions. Moreover, the negative impact of competing reactions is reflected in the total suppression of NH_3 decomposition activity in the presence of CO/H_2 (trace ◇) and the findings obtained in NH_3 temperature-programmed studies in the presence or absence of fuel (Fig. 6).

To further quantify the effect of CO modification of the Rh surface a series of 1% $Rh–Al_2O_3$ catalysts were pretreated for 15 min in 1% CO at 300°C, purged for 45 min in He, and then exposed to 1000 ppm NH_3 in the presence of O_2 or NO, at a range of concentrations at 300°C, and the N_2 production (normalized to the activity of a clean 1% $Rh–Al_2O_3$, to account for NH_3 adsorption and decomposition activity) and total product spectrum monitored. These analyses are summarized in Figs. 11a and 11b.

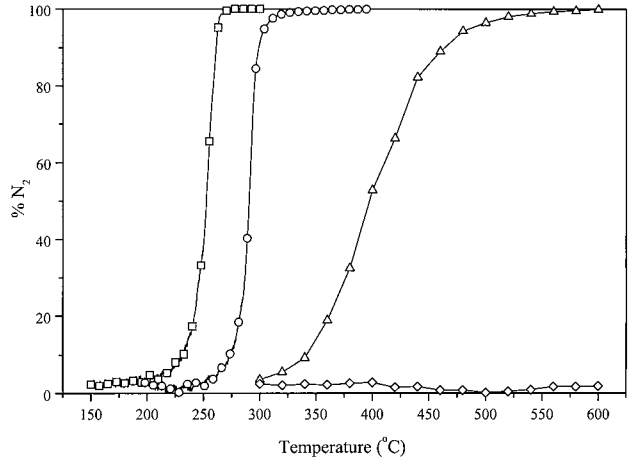

FIG. 10. Comparison of CO/NO, NH_3/NO, and NH_3 decomposition reactions over 1% $Rh–Al_2O_3$. □, N_2 production from the reaction of 1500 ppm NO/5000 ppm CO; ○, N_2 production from the reaction of 1500 ppm NO/1000 ppm NH_3; △, N_2 production from the reaction of 1000 ppm NH_3 in He; ◇, N_2 production from the reaction of 1000 ppm NH_3, 5.35% CO, 3.56% H_2 in He.

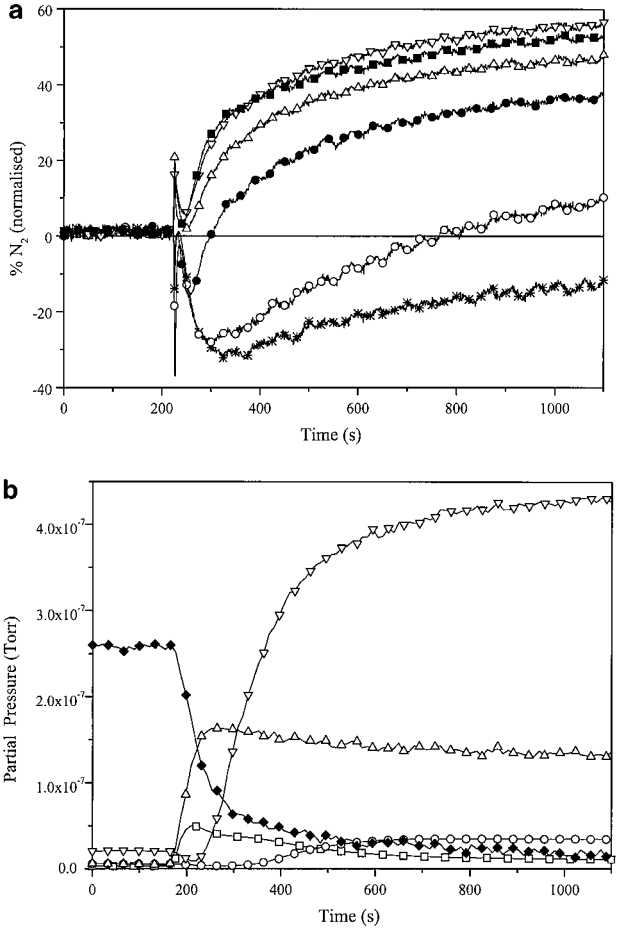

FIG. 11. (a) Normalized N_2 production profiles from the reaction of 1000 ppm NH_3 + oxidant (O_2 or NO as indicated) over a CO-treated 1% $Rh–Al_2O_3$ catalyst at 300°C. ∗, Oxidant-free, i.e., NH_3, decomposition; ○, 100 ppm NO; △, 756 ppm NO; ▽, 1000 ppm NO; ■, 756 ppm O_2; ●, 7550 ppm O_2. (b) Total product profile from the reaction of 1000 ppm NH_3 + 756 ppm O_2 over a CO-treated 1% $Rh–Al_2O_3$ catalyst at 300°C. □, *m/z* 44 (CO_2); ○, *m/z* 30 (NO); △, *m/z* 28 (N_2); ▽, *m/z* 18 (H_2O); ◆, *m/z* 17 (NH_3).

The data confirm the detrimental effect of CO_{ads}-derived species on NH_3 decomposition activity (trace ∗, Fig. 11a), confirming that even in the absence of co-fed fuel components decomposition is unlikely to make any significant contribution to N_2 production. Similarly the activities of all samples showed an initial induction period of lower activity before recovering slowly to the steady-state activities. Significantly, this behavior is most pronounced for the 100 ppm NO, i.e., at the lowest oxidant concentration. Thus we have ascribed these profiles to a two-step process in which there is a dominant initial reaction between the oxidant and adsorbed CO-derived species, followed subsequently by the direct reaction on the cleaned surface between the NH_3 and oxidant.

This premise is clearly illustrated in Fig. 11b, for the reaction of 1000 ppm NH_3 and 756 ppm O_2. On switching in the gas (at 180 s) there is an immediate decrease in NH_3, due to both adsorption and oxidation, but in addition there is a marked CO_2 production which decreases with time. Significantly, the CO_2 profile shows two distinct components, an initial peak followed by slower exponential decay. In addition, comparison of the CO_2 profile with NO production (Fig. 11b, traces □ and ○, respectively) shows NO is not produced for some 200 s postswitch, and that NO "breakthrough" occurs only as CO_2 is seen to follow its exponential decrease. This is consistent with the two-stage removal process for CO_{ads}: the first an initial, rapid oxidation by O_2 and the second via a CO + NO reaction, with the NO being produced *in situ* from NH_3 oxidation. This premise is corroborated by an examination of the N_2 production profile (Fig. 11b, trace △), which also shows an initial peak (some 40 s after the CO_2 peak) before decreasing to steady state, concomitant with increasing NO evolution due to depletion of CO_{ads}.

Given this clear modification of catalyst selectivity by CO adsorption we then examined the effect of CO introduction (5000 ppm) on a standard 1500 ppm NO–1000 ppm NH_3 reaction over 1% Rh–Al_2O_3 catalyst. Thus Fig. 12 confirms that in the absence of fuel the Rh catalyst is capable of quantitative conversion of the NO–NH_3 mixture into N_2. Conversely, on introduction of CO (at 1000 s), N_2 production decreases by approximately 40% (trace ▲). Examination of the respective NO and NH_3 conversion profiles (traces □; and ○, respectively) indicated that while conversion of NO remains >98%, NH_3 conversion quickly decreases to zero, consistent with the stoichiometric decrease in N_2, thereby confirming that in the presence of CO, the reduction of NO by CO is also chemically favored.

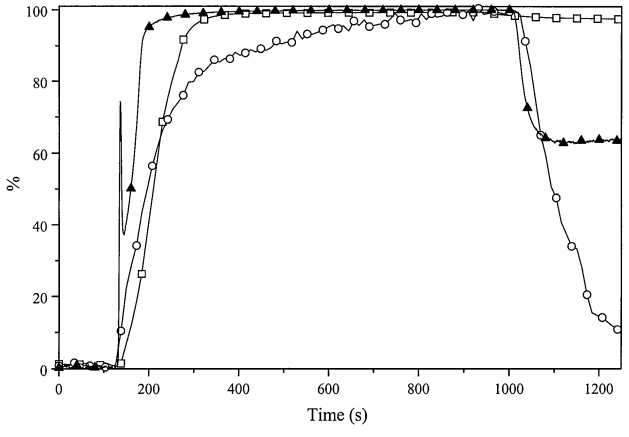

FIG. 12. Effect of the introduction of 5000 ppm of CO on the activity of 1% Rh–Al_2O_3 for the reaction of 1000 ppm NH_3 + 1500 ppm NO at 300°C. □, NO conversion by MS; ○, NH_3 conversion by MS; ▲, total N_2 production by NO_x analysis.

DISCUSSION

The main results from this study can be summarized as follows.

i. Conventional NH_3 oxidation under lean-burn conditions over precious and semiprecious metals affords high activity but in general a low selectivity to N_2. These observations are consistent with the iSCR mechanism of N_2 formation (12, 13, 15, 16, 26–32). However, in the presence of fuel components (CO and H_2) this mechanism is inhibited due to competition for the active surface between NH_3 and particularly CO (cf. Figs. 5 and 6). In addition the exotherm of fuel combustion increases the catalyst temperature, which increases the rate of NO formation (Fig. 1 and (14, 16)), further limiting the effectiveness of the iSCR reaction.

ii. The amount of NO_x observed from the oxidation of NH_3 can be reduced, or even eliminated, when using Rh- or Ir-based catalysts in the presence of CO, H_2, or a combination of CO and H_2 but only under rich conditions. The data obtained (Figs. 2, 9, and 11) are consistent with the following process:

$$yNH_3 + xO_2 \rightarrow \{N_2 + N_2O + NO\} + zH_2O, \quad \text{(a)}$$

$$2NO + 2CO \rightarrow N_2 + 2CO_2, \quad \text{(bi)}$$

and/or

$$2NO + 2H_2 \rightarrow N_2 + 2H_2O, \quad \text{(bii)}$$

and/or

$$\tfrac{3}{2}NO + NH_3 \rightarrow \tfrac{5}{4}N_2 + \tfrac{3}{2}H_2O. \quad \text{(biv)}$$

Figures 3, 4a, 4b, and 8 indicate that step (a) is the limiting one, both kinetically (cf. Figs. 3 and 10) and chemically, because all catalysts facilitated the NO/CO reaction (data not shown), but Pt and Pd could not activate NH_3 under rich conditions. Moreover, the presence of oxygen is critical for N_2 formation over Rh and Ir catalysts in the presence of fuel components, because NH_3 decomposition does not occur under rich conditions (Fig. 10).

iii. Comparison of the $NH_3/CO/O_2$, $NH_3/H_2/O_2$, and $NH_3/CO/H_2/O_2$ reactions (Figs. 8 and 9) shows reaction efficiency to be fuel dependent in the order CO only > H_2 only > CO/H_2 mixture. In addition it has been found that while CO partial pressure has only a mild inhibitory effect with respect to N_2 formation in the $NH_3/CO/O_2$ reaction and CO_{ads} a minor promoter effect in the $NH_3/H_2/O_2$ case, the presence of even trace concentrations of H_2 in the $NH_3/CO/O_2$ can result in a marked decrease in NH_3 conversion/N_2 yield (Fig. 9). This is ascribed to H_2 acting as a scavenging species, which, under certain conditions, removes all available O_2 from the system (see below).

iv. The N_2 selectivity of catalysts is related to the surface state of the precious metal under rich reaction conditions. The use of O_2 as the limiting component in the reaction

controls the reaction exotherm but also establishes competition between the three reductants, with the different species displaying temperature-dependent oxidation selectivity, e.g., for 1% Rh–Al_2O_3 (see Figs. 4a and 4b):

$$2H_2 + O_2 \rightarrow 2H_2O \quad T > 450^\circ C \text{ but } T < 525^\circ C,$$

$$2CO + O_2 \rightarrow 2CO_2 \quad T < 450^\circ C \text{ and } T > 525^\circ C,$$

$$2NH_3 + \tfrac{5}{2}O_2 \rightarrow 2NO + \tfrac{3}{2}H_2O \quad T > 525^\circ C.$$

v. Under the reducing conditions employed, catalyst activity is not limited to oxidation and there is evidence for methanation and CO disproportionation (Figs. 4a and 4b). This accounts for the higher than expected conversions of fuel components under reaction conditions. The presence of CO_{ads} and C_{ads} species on active catalysts is supported by TPD, TPR, and TPO data (Figs. 4a, 4b, 6, 7a, and 7b) where corresponding peaks in H_2O, CH_4, CO, and CO_2 were evident. This premise of atomic-type C species, derived from CO, is also consistent with the recent XPS studies of Rh-based catalysts by Mullins and Overbury (39).

vi. Investigation into the dominant pathway for N_2 production confirms that the initial, and limiting, step of the process is NH_3 oxidation to NO followed by its subsequent reduction. In terms of a power rate expression this latter step may be described as

$$\text{rate of } N_2 \text{ formation} = k(NO)^a(CO)^b + k'(NO)^c(NH_3)^d + k''(NO)^e(H_2)^f.$$

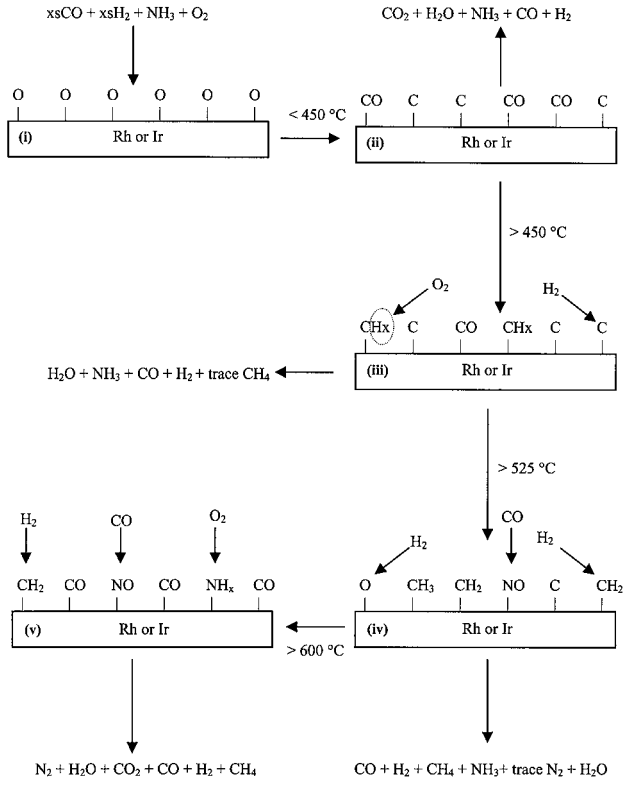

FIG. 13. Model showing the temperature dependence of the surface states and related reaction sequences for catalysts for the selective conversion of NH_3 to N_2 in simulated biogas.

Based on the data obtained (Fig. 10) it is apparent that in the absence of competing reactions the NO/CO reaction is kinetically favored. In addition, when we note the complete suppression of the NH_3/NO reaction by CO (Fig. 12), it is clear that under the conditions employed in this study the CO/NO reaction is both chemically and kinetically preferred.

From the above summary it is evident that the state of the adsorbed species on the catalyst surface is modified *in situ* under reaction conditions by interaction with the gaseous components of the feedstream. It is the nature of these modifications that determines whether or not the catalyst is active in the coupled NH_3 to NO_x to N_2 reaction. We have attempted to summarize these processes in Fig. 13. This enables one to contrast the Rh- or Ir-based catalysts with Pt, Pd. The former materials accumulate CO_{ads} (or C_{ads}) during "lower"-temperature operation, this process being further facilitated by the low O_2 partial pressure (Fig. 13, state ii). This initially results in a partial poisoning of the metal particle for the direct combustion of CO and H_2. Then, as the temperature increases H_2 reacts first with the O of the CO_{ads} to give $C_{ads} + H_2O$ (cf. Figs. 4a, 4b, and 7a) and subsequently with the C_{ads} itself to produce $CH_{X\,ads}$. However, this species can react with $O_{2(g)}$ to produce H_2O and "regenerate" the original C_{ads} site. Hence under these conditions an equilibrium is established between the $CH_{X\,ads}$ and C_{ads} states of the adsorbed carbon with the concomitant scavenging of all available O_2 in the system; this corresponds to Fig. 13, state iii.

This equilibrium explains the inhibition of the NH_3/CO/O_2 reaction by trace levels of H_2 on a partially "cleaned" surface (TPR—Figs. 7a and 9) and the comparative insensitivity of the NH_3/CO/O_2 reaction to increased levels of CO. However at higher temperatures the rate of the C_{ads}-mediated H_2/O_2 reaction is exceeded by that of the direct reaction between C_{ads} and H_2, which results in the gasification of the carbonaceous species as CH_4 (Figs. 4b and 7a; Fig. 13, states iv and v). This process has two important and simultaneous consequences. First, the metal surface is "cleaned" of poisoning carbonaceous moieties, returning it to a fully active state, consistent with the findings of Wild *et al.*, who found that H_2 treatment of coked Rh catalysts at 210°C removed all carbon deposits while the equivalent treatment of Pt yielded no such removal (40). Second, the gasification removes the carbon-modified active site responsible for the scavenging of O_2 by H_2 as outlined previously. This enables the NH_3 to compete for the available O_2 on the clean Rh or Ir surface to produce NO_x, which in turn is reduced by the CO to N_2, as shown in Fig. 13, state v. Finally it should be stressed that once this cleaning process is complete there

is little or no subsequent alteration of the active surface, i.e., further coking. Indeed, previous data have shown that >99.5% conversion of NH_3 to N_2 is possible at high CO/H_2 levels, in the presence of steam for >5 h (14).

In the case of the unselective catalysts ($Pt–Al_2O_3$ and $Pd–Al_2O_3$) no equivalent processes are observed, again consistent with the findings of Wild *et al.* (40). At all temperatures NH_3 and CO conversions are low, and H_2 conversion is correspondingly high. These results for catalysts known to have high CO–NO indicate that they exhibit low N_2 yields because they are unable to selectively activate NH_3 under rich conditions because all the O_2 in the system reacts in the $H_2 + O_2$ reaction.

CONCLUSIONS

The selective oxidation of NH_3 to N_2 in simulated biogas is possible using Rh- and Ir-based catalysts under O_2-limited conditions. These materials display quantitative conversion of NH_3 to N_2 by a coupled NH_3 oxidation to NO and subsequent NO reduction by CO. The key to the success of this methodology is the ability of Rh and Ir to facilitate preferential oxidation of the trace concentrations of NH_3 present in the large excess of fuel. This arises due to the balance of interrelated reactions between CO, H_2, O_2, and NH_3 which result in the *in situ* modification of the catalyst surface.

ACKNOWLEDGMENTS

We are pleased to acknowledge the financial support of ABB-Alstom, DTI, and EPSRC through the FORESIGHT Challenge initiative. Helpful discussions with colleagues at Queens (Mr. I. Burton), Cranfield University (Mr. J. J. Witton, Professor B. Moss, Mr. J. M. Przybylski, and Dr. E. Noordally), and ABB-Alstom (Mr. M. Cannon and Mr. G. Kelsall) are gratefully acknowledged.

REFERENCES

1. "Kyoto Protocol to the United Nations Framework Convention on Climate Change, Kyoto, Japan, 1–10 December 1997."
2. U.S. Environmental Protection Agency. White House Initiative on Global Climate Change. http://www.epa.gov/oppeoee1/globalwarming/actions/solar/index.html and links.
3. Dincer, I., *Renewable Sustainable Energy Rev.* **4**(2), 157 (2000).
4. "Development of Improved Stable Catalysts and Trace Element Capture for Hot Gas Cleaning," DTI/ETSU/Clean Coal Power Generation Group, Project Profile 178, 1996.
5. Obernberger, I., *Biomass Bioenergy* **14**, 33 (1998).
6. Zwinkels, M. F. M., Eloise Heginuz, G. M., Gregertsen, B. H., Sjöström, K., and Järås, S. G., *Appl. Catal. A* **148**, 325 (1997).
7. Lietti, L., Groppi, C., and Ramella, C., *Catal. Lett.* **53**, 91 (1998).
8. Johansson, E. M., and Järås, S. G., *Catal. Today* **47**, 359 (1999).
9. Lietti, L., Ramella, C., Groppi, G., and Forzatti, P., *Appl. Catal. B* **21**, 89 (1999).
10. Johansson, E. M., Berg, M., Kjellström, K., and Järås, S. G., *Appl. Catal. B* **20**, 319 (1999).
11. European Patent 0706 816 A1, assigned to Haldor Topsoe.
12. Amblard, M., Burch, R., and Southward, B. W. L., *Appl. Catal. B* **22**, L159 (1999).
13. Amblard, M., Burch, R., and Southward, B. W. L., *Catal. Today* **59**, 365 (2000).
14. Burch, R., and Southward, B. W. L., British Patent Application 98238879.3 (1998); Burch, R., and Southward, B. W. L., *Chem. Commun.*, 703 (2000).
15. Burch, R., and Southward, B. W. L., *Chem. Commun.*, 1475 (1999).
16. Burch, R., and Southward, B. W. L., *J. Catal.* **195**, 217 (2000).
17. Mojtahedi, W., and Abbasian, J., *Fuel* **74**, 1698 (1995).
18. Simell, P., Kurkela, E., Ståhlberg, P., and Hepola, J., *Catal. Today* **27**, 55 (1996).
19. Gobbina, E. N., Oklany, J. S., and Hughes, R., *Ind. Eng. Chem. Res.* **34**, 3777 (1995).
20. Amann, M., and Lutz, M., *J. Hazardous Mater.* **78**(1–3), 41 (2000).
21. U.S. Environmental Protection Agency, "Tier 2 Emission Standards and Gasoline Regulations" (1999).
22. Zeldovich, J., *Acto Physiochem. USSR* **21**, 577 (1946).
23. Kaspar, J., Clausen, C. A., and Cooper, C. D., *J. Air Waste Manage. Assoc.* **46**, 127 (1996).
24. Heck, R., *Catal. Today* **53**, 519 (1999).
25. Vatcha, S. R., *Eng. Conv. Waste Manage.* **38**, 1327 (1997).
26. Amblard, M., Ph.D. thesis, University of Reading, 1999.
27. Janssen, F. J. J. G., van den Kerkhof, F. M. G., Bosch, H., and Ross, J. R. H., *J. Phys. Chem.* **91**, 5921 (1987).
28. Janssen, F. J. J. G., van den Kerkhof, F. M. G., Bosch, H., and Ross, J. R. H., *J. Phys. Chem.* **91**, 6633 (1987).
29. II'chenko, N. I., and Golodets, G. I., *J.Catal.* **39**, 57 (1975).
30. II'chenko, N. I., and Golodets, G. I., *J.Catal.* **39**, 73 (1975).
31. Curtin, T., O'Regan, F., Deconinck, C., Knuttle, N., and Hodnett, B. K., *Catal. Today* **55**, 189 (2000).
32. Amblard, M., Burch, R., and Southward, B. W. L., *Catal. Lett.* **68**(1–2), 75 (2000).
33. Ramis, G., and Busca, G., *Catal. Today* **28**, 373 (1996).
34. Gallardo Amores, J. M., Sanchez Escribano, V., Ramis, G., and Busca, G., *Appl. Catal.* **B**, 45 (1997).
35. Fritz, A., and Pitchon, V., *Appl. Catal. B* **13**, 1 (1997).
36. Ferri, D., Forni, L., Dekkers, M. A. P., and Nieuwenhuys, B. E., *Appl. Catal. B* **16**, 339 (1998).
37. Farrauto, R. J., and Heck, R. M., *Catal. Today* **51**, 351 (1999).
38. Gavril, D., and Karaiskakis, G., *J. Chromatogr. A* **845**(1, 2), 67 (1999).
39. Mullins, D. R., and Overbury, S. H., *J. Catal.* **188**, 340 (1999).
40. Wild, U., Tescher, D., Schlögl, R., and Paál, Z., *Catal. Lett.* **67**, 93 (2000).